Quantitative Evaluation of Carotid Plaque Composition by In Vivo MRI

T. Saam, M.S. Ferguson, V.L. Yarnykh, N. Takaya, D. Xu, N.L. Polissar, T.S. Hatsukami, C. Yuan

Objective—This study evaluates the ability of MRI to quantify all major carotid atherosclerotic plaque components in vivo.

Methods and Results—Thirty-one subjects scheduled for carotid endarterectomy were imaged with a 1.5T scanner using time-of-flight–, T1-, proton density–, and T2-weighted images. A total of 214 MR imaging locations were matched to corresponding histology sections. For MRI and histology, area measurements of the major plaque components such as lipid-rich/necrotic core (LR/NC), calcification, loose matrix, and dense (fibrous) tissue were recorded as percentages of the total wall area. Intraclass correlation coefficients (ICCs) were computed to determine intrareader and inter-reader reproducibility. MRI measurements of plaque composition were statistically equivalent to those of histology for the LR/NC (23.7 versus 20.3%; $P=0.1$), loose matrix (5.1 versus 6.3%; $P=0.1$), and dense (fibrous) tissue (66.3% versus 64%; $P=0.4$). Calcification differed significantly when measured as a percentage of wall area (9.4 versus 5%; $P<0.001$). Intrareader and inter-reader reproducibility was good to excellent for all tissue components, with ICCs ranging from 0.73 to 0.95.

Conclusions—MRI-based tissue quantification is accurate and reproducible. This application can be used in therapeutic clinical trials and in prospective longitudinal studies to examine carotid atherosclerotic plaque progression and regression. (***Arterioscler Thromb Vasc Biol.* 2005;25:234-239.**)

Key Words: atherosclerosis ■ magnetic resonance imaging ■ carotid artery ■ plaque

Atherosclerosis and its thrombotic complications are the leading cause of morbidity and mortality in industrialized countries. Therefore, the need for new medical therapies and technology to treat and prevent cardiovascular atherosclerotic disease is enormous.

Accurate information of atherosclerotic plaque morphology and plaque composition is necessary to identify the "vulnerable plaques" that are likely to cause embolic events. A noninvasive imaging modality that could provide such information would be an invaluable tool in studies of the relationship between plaque composition/morphology and plaque progression/regression. Furthermore, such imaging techniques may be used in clinical trials to monitor the effects of drugs on diseased arteries.

B-Mode ultrasonography has been used widely in plaque progression/regression trials that involve either lipid-lowering drugs or calcium channel blockers.[1] However, this modality is highly operator dependent, has limited soft tissue contrast, and requires a large number of subjects to detect a significant change in the intima-media thickness.[1] Intravascular ultrasound (IVUS) is used increasingly in atherosclerosis regression/progression trials that study coronary arteries.[2] Although IVUS is highly reproducible[3] and provides tomographic information about the vessel wall,[3] it is an invasive procedure and has limited capacity to discriminate between fibrous and fatty plaques.[4]

Recent publications[5–11] have shown that in vivo MRI can identify the main components of the atherosclerotic plaque such as the lipid-rich/necrotic core (LR/NC), calcification, and hemorrhage. In addition, morphological information about the status of the fibrous cap[12] and the American Heart Association (AHA) lesion type[13] can be obtained noninvasively. Moreover, the tomographic orientation of MRI enables the full cross-sectional view of the vessel wall, which can be measured accurately[14] and reproducibly.[15] It has been demonstrated that ex vivo MRI of endarterectomy specimen is able to identify[16] and quantify[17,18] plaque components with high diagnostic accuracy. This study is aimed at evaluating the ability of MRI to quantify all major carotid atherosclerotic plaque components in vivo, using histology as the standard of reference.

Methods

Study Population

Data sets were obtained from 40 consecutively selected subjects (mean age 68 years; SD 9 years; 2 females) scheduled for carotid endarterectomy at either the University of Washington Medical Center or Veterans Administration Puget Sound Health Care System.

Original received July 7, 2004; final version accepted October 26, 2004.

From the Department of Radiology (T.S., M.S.F., V.L.Y., N.T., D.X., C.Y.), University of Washington; Mountain-Whisper-Light Statistical Consulting (N.L.P.); and the Department of Surgery, University of Washington, and VA Puget Sound Health Care System (T.S.H.), Seattle, Wash.

Correspondence to Chun Yuan, Professor, Department of Radiology, 1959 NE Pacific St, Box 357115, Seattle, WA 98195. E-mail cyuan@u.washington.edu

Arterioscler Thromb Vasc Biol. **is available at http://www.atvbaha.org** **DOI: 10.1161/01.ATV.0000149867.61851.31**

TABLE 1. Tissue Classification Criteria

	TOF	T1W	PDW	T2W
LR/NC with				
No or little hemorrhage	o	o/+	o/+	−/o
Fresh hemorrhage	+	+	−/o	−/o
Recent hemorrhage	+	+	+	+
Calcification	−	−	−	−
Loose matrix	o	−/o	+	+
Dense (fibrous) tissue	−	o	o	o

The classification into the subgroups is based on the following SIs relative to adjacent muscle: +, hyperintense; o, isointense; −, hypointense.

Nine subjects were excluded because of either poor image quality (n=7) or the disruption of the histological specimen during excision or processing (n=2), resulting in 31 evaluated subjects. Institutional review boards of each facility approved the consent forms and study protocols. Selected subjects either had symptomatic carotid disease on the side of a >50% internal carotid artery (ICA) stenosis (by duplex), or an asymptomatic >80% ICA stenosis. Subjects were considered symptomatic if they had a history of transient ischemic attack, amaurosis fugax, or stroke attributed to the distribution of the index carotid artery within 120 days before the MRI scan. Subjects underwent a carotid artery MRI examination within 1 week before their surgical procedure.

MRI Protocol

Subjects were imaged using 1.5T MR scanners (Signa Horizon EchoSpeed; General Electric Health Care) and phased-array surface coils (Pathway MRI, Inc.). Fast spin-echo (FSE)–based T1-weighted (T1W), proton density–weighted (PDW), and T2-weighted (T2W) images as well as time-of-flight (TOF) images of bilateral carotid arteries were obtained using a previously published standardized protocol.[19] The scan was centered on the bifurcation of the operative side. In most cases, this scan covered the complete atherosclerotic plaque. Average scan time was 35 to 45 minutes. All images were obtained using a field-of-view of 13 to 16 cm, matrix size of 256, slice thickness of 2 mm (1 mm for 3D TOF) and 2 signal averages. A zero-filled Fourier transform was used to reduce pixel size (0.25×0.25 or 0.31×0.31 mm^2) and to minimize partial-volume artifacts.

Image Review

Before review, an image-quality rating (5-point scale: 1=poor and 5=excellent) for each contrast weighting was assigned to all MR images[9] by a radiologist (T.S.). Imaging locations with an image quality ≤2 in T1W, T2W, or TOF (indicating severe blurring attributable to subject motion or low signal-to-noise ratio) were excluded from the study. TOF images were acquired every millimeter, whereas FSE images were acquired every 2 mm. Because of the different slice distance and thus the higher number of TOF images, only every second TOF image (the one with the best anatomic match with the corresponding FSE images) was used. For each imaging location, 4 contrast-weighted images were reviewed. Average review time was 30 to 60 minutes per artery.

All MR images were examined by a radiologist (T.S.) who was blinded to the histology findings. To assess intrareader and interreader reproducibility, MR images of 20 randomly selected subjects were re-evaluated 9 months after the initial review by 2 reviewers (T.S. and N.T.).

Area measurements of the lumen, outer wall, and the tissue components were obtained using the custom-designed imaging analysis tool QVAS.[20] The outer wall boundary included lumen and wall area. Wall area was calculated as the difference between outer wall boundary and lumen area.

The tissue type classification scheme (Table 1) was derived from our experience of reviewing MR images[9,11] and an extensive literature review of atherosclerosis publications.[5–8,16,18] All signal intensities (SIs) are relative to the adjacent sternocleidomastoid muscle. Five tissue types were identified.

1. The LR/NC is generally located in the bulk of the plaque and is isointense to hyperintense on T1W and PDW images. However, depending on the amount and age of hemorrhage present, the LR/NC has varied SIs on T2W and TOF images (Table 1).
2. Areas of hemorrhage were identified as described previously by Chu et al.[11] Briefly, fresh intraplaque hemorrhage appears as a hyperintense signal on T1W and TOF images and as an isointense signal on T2W/PDW images. Recent hemorrhage is identified by a hyperintense signal on all 4 contrast weightings. Area measurements of hemorrhage collected in this study combine area measurements of fresh and recent hemorrhage.
3. Calcification is characterized by defined areas with a hypointense signal on all 4 weightings.
4. Loose matrix is hyperintense on T2WI and PDWI, isointense to hypointense on T1WI and isointense on TOF images.
5. Dense fibrous tissue is hypointense on TOF images and isointense on T1W, PDW, and T2W images. The area of dense (fibrous) tissue was calculated by subtracting the areas of LR/NC, calcification, and loose matrix from the total wall area.

Histology Processing and Criteria

Carotid endarterectomy specimens were fixed in 10% neutral-buffered formalin, decalcified, and embedded en bloc in paraffin. Serial sections (10-μm thick) were taken every 1 mm in the common carotid artery, every 0.5 mm in the ICA throughout the length of the specimen, and stained with hematoxylin-eosin and Mallory's Trichrome. Histological classification of the specimens was performed using criteria established by the AHA Committee on Vascular Lesions. A reviewer (M.S.F; unaware of the MRI data) used standard histopathologic criteria to examine all histology sections.[21,22]

MRI and Histology Matching

The process of matching images to histology used landmarks such as the relative distance from the common carotid bifurcation and gross morphological features such as lumen size and shape, wall size and shape, plaque configuration, as well as calcifications (Figure 1). Shrinkage of the specimens because of processing is inconsistent throughout the specimen, and multiple internal landmarks were required for accurate matching.[9] Histology was sectioned every 0.5 to 1 mm, and therefore, 1 to 4 histological sections could be matched to 1 MR imaging location (slice thickness 2 mm). If >1 histology section matched to 1 MR imaging location, we calculated the mean of the areas measured in the multiple histology sections and compared it with the corresponding MR image. All MR image locations that could be matched to corresponding histology sections were included in the study. In total, 273 MR image locations (5 to 10 locations per subject; mean 6.9; SD=1.6; 1 artery per subject) were matched and compared with the corresponding 600 histological sections from serially sectioned endarterectomy specimens (Figure 1).

Data Analysis

Sensitivity, specificity, and Cohen's kappa (κ; based on MRI locations as the unit of observation) were calculated for all plaque components independently of their size and separately for plaque components >2 mm^2, using histology as a gold standard. For MRI results to agree with histology results, we required that the components identified by MRI were present in the histology section that was matched to the MR imaging location. The 2 mm^2 threshold for plaque components is comparable to the one used by Chiesa et al[23] and takes into account the limited spatial resolution of in vivo MRI.

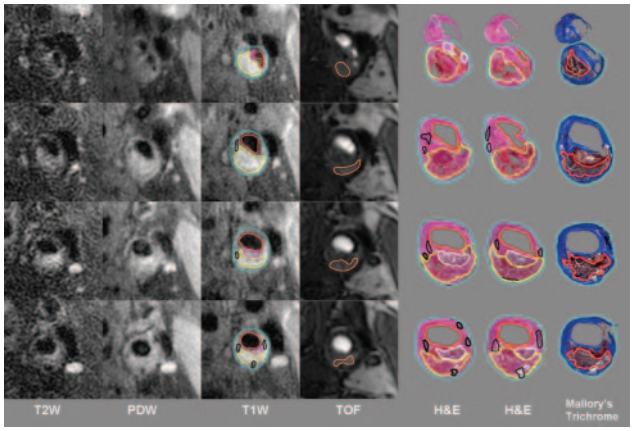

Figure 1. Example of histological validation of MRI at 4 consecutive locations spanning the bifurcation. Multiple histological sections (at 0.5 to 1.0 mm separation) generally correspond to each 2-mm-thick MR image. Contours have been drawn for lumen (red), outer wall (cyan), LR/NC (yellow), calcification (black), loose matrix (pink/white), and hemorrhage (orange). H&E indicates hematoxylin-eosin.

Because of the multiple locations for each artery within a patient, and the possibility of statistical dependence, the 95% confidence intervals (CIs) for sensitivity, specificity, and Cohen's κ were calculated with the bootstrap method (with 10 000 resamples).[24]

To lessen the impact of mismatch between MRI and histology and to accommodate for possible statistical dependence of multiple locations per artery, we used the artery as the unit of observation for all calculations based on continuous variables, such as area measurements or percentages. Artery-based data were normalized by dividing the sum of all areas/percentages across locations by the number of locations (or sections for histology) per subject. As an initial estimate of accuracy of prediction of MRI area measurements compared with histology, the mean difference (bias) between the MRI and histology was calculated (according to the method described by Bland and Altman[25] [Figure 2]) for the plaque components.

Overall agreement between area measurements was estimated by Pearson correlation coefficients (r) to accommodate the shrinkage and distortion that occurs during histological processing. Each plaque component was calculated as percentage of the vessel wall [%plaque component=(area plaque component/wall area) ·100%]. The paired t test was used to compare the plaque composition as percentage of the vessel wall between MRI and histology.

To determine intrareader and inter-reader reproducibility measurements, the intraclass correlation coefficient (ICC) with 95% CI was calculated to measure the level of agreement between 2 measurements repeated within subjects compared with the variation in the measurement across subjects.

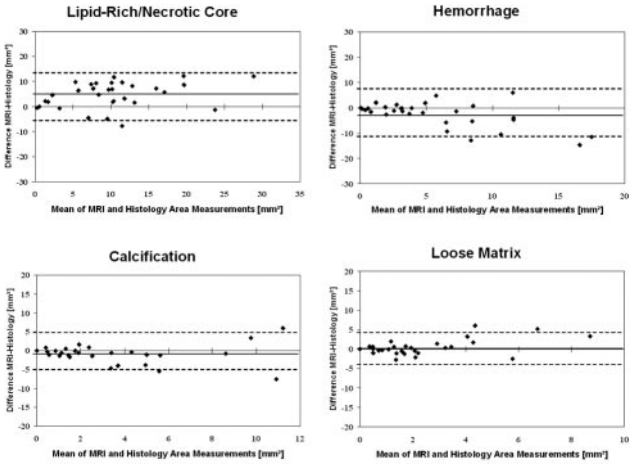

Figure 2. Bland–Altman plots for area measurements (mean per location) of the plaque components (n=31 arteries). Histology consistently underestimates the size of the LR/NC and of loose fibrous matrix, with increasing bias and variance at larger sizes. There is no bias for calcification measurements, whereas hemorrhagic areas are larger by histology, showing increasing bias with size.

Results

Sensitivity and Specificity

Overall plaque component sensitivity ranged from 64% to 92% (Table 2). Plaque component specificity ranged from 65% to 86%. When only areas >2 mm^2 were considered, sensitivity and specificity were 95% and 76% for the LR/NC, 84% and 91% for calcification, 87% and 84% for hemorrhage, and 79% and 77% for loose matrix. This resulted in Cohen's κ values of 0.73 for the LR/NC, 0.75 for calcification, 0.71 for hemorrhage, and 0.53 for loose matrix. Table 2 also indicates the number of locations displaying a specified feature as determined by histology. Of note, 38 of 104 (37%) of all loose matrix areas found in this study were <2 mm^2, compared with only 13% of LR/NC areas, 21% of calcification areas, and 17% of hemorrhage areas.

Correlation Analysis

There was a strong correlation between MRI and histology area measurements (mean per location) for lumen (r=0.81; P<0.001), wall (r=0.84; P<0.001), outer wall (r=0.82; P<0.001), LR/NC (r=0.75; P<0.001), calcification (r=0.74; P<0.001), and loose matrix (r=0.70; P<0.001) (Table 3). There was a moderate correlation between MRI and histology measurements of dense (fibrous) tissue (r=0.55; P=0.001) and a moderate to strong correlation between measurements of hemorrhage (r=0.66; P<0.001).

Plaque Composition and Plaque Shrinkage

Figure 3 shows the mean prevalence of plaque components as percent wall area of the 31 arteries measured by histology and by MRI. Plaque composition calculated as percentage of the vessel wall was comparable for MRI and histology for the LR/NC (23.7 versus 20.3%; P=0.1), loose matrix (5.1 versus 6.3%; P=0.1), and dense (fibrous) tissue (66.3 versus 64%; P=0.4). Calcifications appeared to be underestimated by MRI (5.0% by MRI but 9.4% by histology; P<0.0001). However, area measurements of calcification did not differ significantly (mean area per location 2.7 mm^2 by MRI and 3.5 mm^2 by histology; mean difference±SD −0.8±2.8 mm^2; P=0.1).

Using histology as the gold standard, MRI measurements of lumen, wall, LR/NC, loose matrix, and dense (fibrous) tissue were found to be consistently overestimated (Figure 2). MRI showed a systematic underestimation of the hemorrhage area (4.3 mm^2 by MRI and 6.7 mm^2 by histology; mean difference±SD −2.4±4.9 mm^2; P=0.008). This underestimation increased with the size of hemorrhage measured (Figure 2).

TABLE 2. Sensitivity and Specificity Based on 214 Locations*

Tissue Type	Sensitivity/Specificity (all areas)	Sensitivity/Specificity (areas>2 mm^2 by histology)	κ (95% CI)
LR/NC	92%/65% (n=165)	95%/76% (n=144)	0.73 (0.62–0.82)
Calcification	76%/86% (n=123)	84%/91% (n=97)	0.75 (0.66–0.84)
Hemorrhage	82%/77% (n=158)	87%/84% (n=131)	0.71 (0.61–0.80)
Loose matrix	64%/72% (n=104)	79%/77% (n=66)	0.53 (0.41–0.64)

*No. of locations with the specified tissues component is noted in parentheses.

Reproducibility

Intrareader reproducibility (ICC; 95% CI) was excellent for area measurements of LR/NC (0.89; 0.75 to 0.95) and calcification (0.9; 0.77 to 0.96), and good for hemorrhage (0.74; 0.45 to 0.89) and for loose matrix (0.79; 0.54 to 0.91). Inter-reader reproducibility (ICC; 95% CI) was excellent for area measurements of LR/NC (0.92; 0.82 to 0.97) and calcification (0.95; 0.88 to 0.98), and good for hemorrhage (0.73; 0.44 to 0.88) and for loose matrix (0.79; 0.55 to 0.91).

Discussion

This study demonstrates the capabilities of in vivo MRI to quantify all the major components of the advanced human carotid atherosclerotic plaque. Each plaque component measured in this study provides unique information about the status of atherosclerotic disease: LR/NC size may play an important role in the pathogenesis of plaque rupture;[26] intraplaque hemorrhage may stimulate the progression of atherosclerotic plaque;[27] calcification can provide a general indication of plaque burden;[28] and loose matrix is involved in coronary plaque healing in subjects with silent plaque rupture,[29] which can result in increased stenosis.[29] In vivo identification and quantification of those atherosclerotic plaque components enables us to study the underlying mechanisms of atherosclerotic disease in humans prospectively. This may help us to (1) better understand basic concepts of atherosclerotic disease progression/regression in humans, (2) monitor antiatherosclerotic treatment effects more efficiently, (3) develop new antiatherosclerotic treatment strategies, and (4) improve and develop strategies to prevent atherosclerotic disease.

MRI tissue characterization of complex human carotid atherosclerotic plaques can be accomplished in vivo with high sensitivity (79% to 95%) and moderate to high specificity (76% to 91%) for plaque components >2 mm^2 with Cohen's κ ranging from 0.53 to 0.75 (Table 2). Sensitivity and specificity decreased slightly for all components if areas <2 mm^2 were included. Overall, sensitivity and specificity were slightly lower than in an ex vivo study by Shinnar et al[16] that used 9.4T MRI. This is most likely attributable to the inferior spatial resolution of 1.5T MRI, and we expect significant improvement of sensitivity and specificity with improvements in hardware, particularly with the higher resolution expected from 3T MRI.

The correct identification of each plaque component is based on signal intensity relative to the adjacent muscle. The additional challenge for quantification of plaque components is its accurate delineation of boundaries. The results of this study suggest that both MRI reviewers had few difficulties in delineating the boundaries of the LR/NC and calcification, resulting in excellent intrareader and inter-reader reproducibility. Furthermore, the correlation of MRI to histology for area measurements of the LR/NC and calcification were high and (Table 3) comparable to those obtained for lumen and wall areas.

Boundaries of hemorrhage are at times not clearly demarcated because hemorrhage diffuses into the LR/NC. Loose matrix areas were generally small in size, and their often

TABLE 3. Artery-Based Correlation Between MRI and Histology (Average Area per Location)

	No. of Measurements	r	*P*
Lumen	31	0.81	<0.001
Wall	31	0.84	<0.001
Outer wall	31	0.82	<0.001
LR/NC	31	0.75	<0.001
Calcification	31	0.74	<0.001
Hemorrhage	31	0.66	<0.001
Loose matrix	31	0.70	<0.001
Dense (fibrous) tissue	31	0.55	0.001

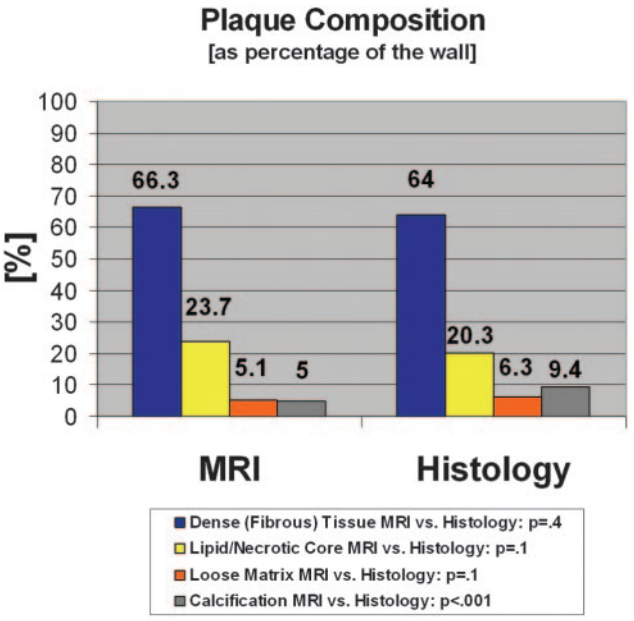

Figure 3. Plaque composition calculated as the percentage of the vessel wall area, calculated per artery, and then averaged across all arteries for MRI and histology.

juxtaluminal location complicates differentiation from flow artifacts. Therefore, intrareader and inter-reader reproducibility of the MRI-based review for hemorrhage and loose matrix was slightly lower than that for LR/NC and calcification. The correlation of MRI to histology for area measurements of loose matrix and hemorrhage was lower than that for area measurements of LR/NC and calcification.

Dense (fibrous) tissue was indirectly calculated by subtracting specified tissue types from the wall area. Therefore, false-positive or false-negative classification of other tissue types and any measurement errors of areas could bias the calculation of areas of dense (fibrous) tissue. This might explain the moderate correlation of MRI to histology for area measurements of dense (fibrous) tissue areas.

Overall, the findings in this study for the quantification of plaque components are comparable to a recent ex vivo MRI study[18] that used endarterectomy specimen to quantify plaque components. The authors of the latter study reported good to excellent results for correct classification of necrosis and calcification but had difficulty with correctly classifying loose connective tissue and fibrous tissue.[18]

The composition of the plaque calculated as proportion of the vessel wall area did not differ significantly between MRI and histology for the LR/NC (23.7 versus 20.3%; $P=0.1$), loose matrix (5.1 versus 6.3%; $P=0.1$), and dense (fibrous) tissue (66.3 versus 64%; $P=0.4$; Figure 3). Calcification as percentage of the vessel wall appeared to be underestimated by MRI (5.0% by MRI but 9.4% by histology; $P<0.001$). However, area measurements of calcification did not differ significantly (2.7 versus 3.5 mm^2; $P=0.1$). There are 2 possible reasons for the underestimation of calcification by MRI: (1) calcification may shrink less than other components during histological processing, and (2) MRI possibly underestimates areas with hypointense signal because of signal averaging of voxels that only partially contain calcification.

As demonstrated in Table 1, no single contrast weighting was used to identify the different plaque components accurately. Rather, combined information from TOF, T1W, PDW, and T2W images provided the most comprehensive evaluation. The criteria for identifying the LR/NC was slightly modified from previously published work.[9] Although we found that the majority of the LR/NC regions are hyperintense on T1W images, LR/NCs containing little or no hemorrhage appear more isointense than hyperintense on T1W images. Furthermore, consistent with previous reports[8,9,16] in the literature, many of the LR/NC regions appeared hypointense to isointense on PDW and T2W images. However, we found that LR/NCs in other regions, which contained recent hemorrhage by histology, were hyperintense on PDW and T2W images. This study provided further evidence that LR/NCs can potentially display a variety of different signal features, depending on the amount and the age of hemorrhage within the LR/NC (Table 1).

Limitations

Rigorous quantitative comparison of in vivo MR images and histology sections requires careful attention to registration of cross-sections. Because the MRI slice thickness (2 mm) is greater than that of the histological section (10 μm), the MR image represents a composite of 200 histology sections. Thus, in complex specimens containing lesions that may change significantly in size or composition from section to section, it can be difficult to obtain precise coregistration. To lessen the impact of mismatch, correlation analysis was performed by using the sum of areas per artery (for each plaque component) divided by the number of locations rather than comparing area measurements on a section-by-section basis. However, for the calculation of sensitivity and specificity, location-based data were used. Therefore, mismatch between MRI and histology decreased any values given for sensitivity and specificity compared with a calculation of these values on the basis of perfect (true) registration.

Histology specimens were obtained from subjects undergoing carotid endarterectomy. Thus, the incidence of pathology was high, and the atherosclerotic lesions were advanced and complex. It would be desirable to substantiate the results by the examination of specimens with less severe atherosclerotic disease. Although specimens could be obtained by autopsy studies, MRI in vivo scans are rarely available for comparison, and ex vivo MRI scans of excised autopsy tissues have other limitations, such as a potential change in tissue contrast resulting from tissue degradation and dehydration.[16]

Only MRI exams of at least average image quality were considered for the review, resulting in the exclusion of 7 arteries from analysis. Because of recent improvements in the imaging protocols, such as the time-efficient multislice double inversion recovery[30] and the contrast-enhanced images with quadruple inversion recovery,[31] the number of exclusions attributable to poor image quality is lower in our current studies and should further decline with improvements in pulse sequence design and in hardware (eg, higher-field MRI).

Conclusions

The results of this study revealed good agreement between in vivo MRI and histology for quantitative measurements of the main plaque components such as LR/NC, calcification, loose matrix, and hemorrhage. Furthermore, the results have shown that quantification of the main plaque components is feasible, with good to excellent intrareader and inter-reader reproducibility. MRI-based tissue quantification can be used in therapeutic clinical trials and in prospective longitudinal studies to examine carotid atherosclerotic plaque progression and regression.

Acknowledgments

This work is supported in part by grants from the National Institutes of Health R01HL56874 and R01HL072262 and from Pfizer, Inc. The authors wish to acknowledge Andrew An Ho for his help in preparing this manuscript.

References

1. O'Leary DH, Polak JF. Intima-media thickness: a tool for atherosclerosis imaging and event prediction. *Am J Cardiol.* 2002;90:18L–21L.
2. Nissen SE. IVUS is redefining atherosclerotic disease. *Am J Manag Care.* 2003;(suppl):2–3.
3. Nissen SE. IVUS is redefining atherosclerotic disease. *Am J Manag Care.* 2003;(suppl):2–3.

4. Hiro T, Leung CY, De Guzman S, Caiozzo VJ, Farvid AR, Karimi H, Helfant RH, Tobis JM. Are soft echoes really soft? Intravascular ultrasound assessment of mechanical properties in human atherosclerotic tissue. *Am Heart J*. 1997;133:1–7.
5. Coombs BD, Rapp JH, Ursell PC, Reilly LM, Saloner D. Structure of plaque at carotid bifurcation: high-resolution MRI with histological correlation. *Stroke*. 2001;32:2516–2521.
6. Fayad ZA, Fuster V. Characterization of atherosclerotic plaques by magnetic resonance imaging. *Ann N Y Acad Sci*. 2000;902:173–186.
7. Serfaty JM, Chaabane L, Tabib A, Chevallier JM, Briguet A, Douek PC. Atherosclerotic plaques: classification and characterization with T2-weighted high-spatial-resolution MR imaging—an in vitro study. *Radiology*. 2001;219:403–410.
8. Toussaint JF, LaMuraglia GM, Southern JF, Fuster V, Kantor HL. Magnetic resonance images lipid, fibrous, calcified, hemorrhagic, and thrombotic components of human atherosclerosis in vivo. *Circulation*. 1996;94:932–938.
9. Yuan C, Mitsumori LM, Ferguson MS, Polissar NL, Echelard D, Ortiz G, Small R, Davies JW, Kerwin WS, Hatsukami TS. In vivo accuracy of multispectral magnetic resonance imaging for identifying lipid-rich necrotic cores and intraplaque hemorrhage in advanced human carotid plaques. *Circulation*. 2001;104:2051–2056.
10. Yuan C, Kerwin WS, Ferguson MS, Polissar N, Zhang S, Cai J, Hatsukami TS. Contrast-enhanced high resolution MRI for atherosclerotic carotid artery tissue characterization. *J Magn Reson Imaging*. 2002;15:62–67.
11. Chu B, Kampschulte A, Ferguson MS, Kerwin WS, Yarnykh VL, O'Brien KD, Polissar NL, Hatsukami TS, Yuan C. Hemorrhage in the atherosclerotic carotid plaque: a high-resolution MRI study. *Stroke*. 2004;35:1079–1084.
12. Hatsukami TS, Ross R, Polissar NL, Yuan C. Visualization of fibrous cap thickness and rupture in human atherosclerotic carotid plaque in vivo with high-resolution magnetic resonance imaging. *Circulation*. 2000;102:959–964.
13. Cai JM, Hatsukami TS, Ferguson MS, Small R, Polissar NL, Yuan C. Classification of human carotid atherosclerotic lesions with in vivo multicontrast magnetic resonance imaging. *Circulation*. 2002;106:1368–1373.
14. Luo Y, Polissar N, Han C, Yarnykh V, Kerwin WS, Hatsukami TS, Yuan C. Accuracy and uniqueness of three in vivo measurements of atherosclerotic carotid plaque morphology with black blood MRI. *Magn Reson Med*. 2003;50:75–82.
15. Kang X, Polissar NL, Han C, Lin E, Yuan C. Analysis of the measurement precision of arterial lumen and wall areas using high-resolution MRI. *Magn Reson Med*. 2000;44:968–972.
16. Shinnar M, Fallon JT, Wehrli S, Levin M, Dalmacy D, Fayad ZA, Badimon JJ, Harrington M, Harrington E, Fuster V. The diagnostic accuracy of ex vivo MRI for human atherosclerotic plaque characterization. *Arterioscler Thromb Vasc Biol*. 1999;19:2756–2761.
17. Morrisett J, Vick W, Sharma R, Lawrie G, Reardon M, Ezell E, Schwartz J, Hunter G, Gorenstein D. Discrimination of components in atherosclerotic plaques from human carotid endarterectomy specimens by magnetic resonance imaging ex vivo. *Magn Reson Imaging*. 2003;21:465–474.
18. Clarke SE, Hammond RR, Mitchell JR, Rutt BK. Quantitative assessment of carotid plaque composition using multicontrast MRI and registered histology. *Magn Reson Med*. 2003;50:1199–1208.
19. Yuan C, Mitsumori LM, Beach KW, Maravilla KR. Carotid atherosclerotic plaque: noninvasive MR characterization and identification of vulnerable lesions. *Radiology*. 2001;221:285–299.
20. Kerwin WS, Han C, Chu B, Xu D, Luo Y, Hwang JN, Hatsukami TS, Yuan C. A quantitative vascular analysis system for evaluation of atherosclerotic lesions by MRI. In: *Medical Image Computing and Computer-Assisted Intervention-MICCAI 2001*. Berlin, Germany: Springer; 2001:786–794.
21. Stary HC, Chandler AB, Dinsmore RE, Fuster V, Glagov S, Insull W Jr, Rosenfeld ME, Schwartz CJ, Wagner WD, Wissler RW. A definition of advanced types of atherosclerotic lesions and a histological classification of atherosclerosis. A report from the Committee on Vascular Lesions of the Council on Arteriosclerosis, American Heart Association. *Circulation*. 1995;92:1355–1374.
22. Stary HC. Natural history and histological classification of atherosclerotic lesions: an update. *Arterioscler Thromb Vasc Biol*. 2000;20:1177–1178.
23. Chiesa G, Rigamonti E, Monteggia E, Parolini C, Marchesi M, Miragoli L, Grotti A, Maggioni F, Lorusso V, Sirtori CR. Evaluation of a soft atherosclerotic lesion in the rabbit aorta by an invasive IVUS method versus a non-invasive MRI technology. *Atherosclerosis*. 2004;174:25–33.
24. Efron B, Tibshirani RJ. *An Introduction to the Bootstrap*. London, England: Chapman and Hall; 1993.
25. Bland JM, Altman DG. Statistical methods for assessing agreement between two methods of clinical measurement. *Lancet*. 1986;1:307–310.
26. Ravn HB, Falk E. Histopathology of plaque rupture. *Cardiol Clin.* 1999;17:263–270.
27. Kolodgie FD, Gold HK, Burke AP, Fowler DR, Kruth HS, Weber DK, Farb A, Guerrero LJ, Hayase M, Kutys R, Narula J, Finn AV, Virmani R. Intraplaque hemorrhage and progression of coronary atheroma. *N Engl J Med*. 2003;349:2316–2325.
28. Burke AP, Weber DK, Kolodgie FD, Farb A, Taylor AJ, Virmani R. Pathophysiology of calcium deposition in coronary arteries. *Herz*. 2001;26:239–244.
29. Burke AP, Kolodgie FD, Farb A, Weber DK, Malcom GT, Smialek J, Virmani R. Healed plaque ruptures and sudden coronary death: evidence that subclinical rupture has a role in plaque progression. *Circulation*. 2001;103:934–940.
30. Yarnykh VL, Yuan C. Multislice double inversion-recovery black-blood imaging with simultaneous slice reinversion. *J Magn Reson Imaging*. 2003;17:478–483.
31. Yarnykh VL, Yuan C. T1-Insensitive flow suppression using quadruple inversion-recovery. *Magn Reson Med*. 2002;48:899–905.